DOI: 10.1002/chem.200500097

Homo-/Heterotrinuclear Mixed-Valent Oxo-Centered Iron/Nickel Clusters—Mössbauer Studies on Internal Electron-Exchange Processes**

Rolf W. Saalfrank,*[a] Andreas Scheurer,[a] Uwe Reimann,[a] Frank Hampel,[a] Christian Trieflinger,[b] Michael Büschel,[b] Jörg Daub,*[b] Alfred X. Trautwein,*[c] Volker Schünemann,[d] and Veaceslav Coropceanu[e]

Abstract: In a one-pot reaction of *N*-(5-methylthiazole-2-yl)-thiazole-2-carboxamide HL^2 (**3**) with iron(II) acetate in air, the homotrinuclear heteroleptic mixed-valent oxo-centered iron cluster $[Fe^{II}Fe^{III}_2O(L^2)_3(OAc)_3]$ (**4**) was formed. Exchange of iron(II) in **4** by nickel(II) afforded the heteronuclear cluster $[Ni^{II}Fe^{III}_2O(L^2)_3(OAc)_3]$ (**6**). To obtain crystals suitable for X-ray structure analyses, in **4** and **6**, the OAc^- co-ligands were exchanged by OBz^- ligands to give $[Fe^{II}Fe^{III}_2O(L^2)_3(OBz)_3]$ (**5**) and $[Ni^{II}Fe^{III}_2O(L^2)_3(OBz)_3]$ (**7**). The complexes **5** and **7** are isostructural and made up of three ditopic, tridentate ligands $(L^2)^-$ and three bridging benzoate co-ligands, which fix the three metal ions in the corners of a triangle with an μ_3-O^{2-} ion in the center. The mixed-valent character of **4**–**7**, their intramolecular electron-exchange processes, and their redox properties were studied by variable-temperature Mössbauer spectroscopy and cyclic voltammetry.

Keywords: electron exchange · iron · mixed valence · Moessbauer spectroscopy · trinuclear

Introduction

Design and construction[1] of supramolecular organic/inorganic structures that exhibit novel properties[2] are of current interest. For example, we reported on rectangular tetrametallic [2×2] grids $[M_4(L^1)_8]$ (**1**)[3] (Scheme 1).

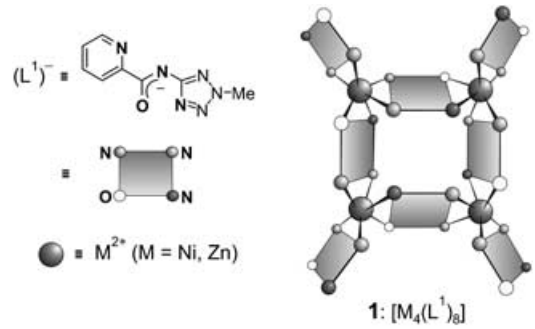

Scheme 1. Schematic presentation of $[M_4(L^1)_8]$ (**1**).

Formal replacement of the pyridine and tetrazole heterocycles in $(L^1)^-$ by thiazole rings led to ligand $(L^2)^-$. The geometric requirements of $(L^1)^-$ and $(L^2)^-$ are pretty much alike; however, when $(L^2)^-$ was treated with zinc acetate in methanol, we isolated the oxo-centered tetrazinc complex $[Zn_4O(L^2)_4(OAc)_2]$ (**2**)[4] (Scheme 2).

Results and Discussion

Synthesis: Herein we report on the reaction of HL^2 (**3**) in fluorobenzene and under aerobic conditions with iron(II)

[a] Prof. Dr. R. W. Saalfrank, Dr. A. Scheurer, Dr. U. Reimann, Dr. F. Hampel
Institut für Organische Chemie der Universität Erlangen-Nürnberg
Henkestrasse 42, 91054 Erlangen (Germany)
Fax: (+49) 9131-852-1165
E-mail: saalfrank@chemie.uni-erlangen.de

[b] Dr. C. Trieflinger, Dr. M. Büschel, Prof. Dr. J. Daub
Institut für Organische Chemie der Universität Regensburg
93040 Regensburg (Germany)

[c] Prof. Dr. A. X. Trautwein
Institut für Physik der Medizinischen Universität Lübeck
23538 Lübeck (Germany)

[d] Prof. Dr. V. Schünemann
Fachbereich Physik, Technische Universität Kaiserslautern
67663 Kaiserslautern (Germany)

[e] Dr. V. Coropceanu
School of Chemistry and Biochemistry
Georgia Institute of Technology
Atlanta, GA 30332–0400 (USA)

[**] Chelate Complexes, Part 29. Part 28: R. W. Saalfrank, T. Nakajima, N. Mooren, A. Scheurer, H. Maid, F. Hampel, C. Trieflinger, J. Daub, *Eur. J. Inorg. Chem.* **2005**, 1149–1153.

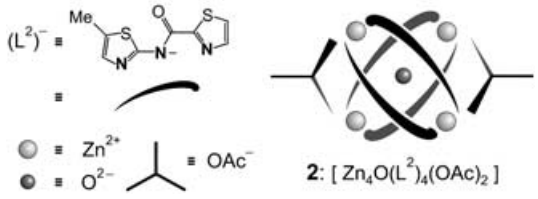

Scheme 2. Schematic presentation of $[Zn_4O(L^2)_4(OAc)_2]$ (**2**).

acetate,[5] which yields the deep violet microcrystalline product **4**, which in turn can be converted to **5**–**7** (Scheme 3). It is worth noting that the *asymmetrically* substituted mixed-valent μ_3-oxo centered trinuclear complexes **4**–**7** are the first of this type.

On the basis of the analytical data and the FAB mass spectrum, **4** was identified as an oxo-triiron chelate complex of the composition $[Fe_3O(L^2)_3(OAc)_3]$ with a metal-to-ligand-to-co-ligand ratio (M:L:co-L) of 1:1:1.[6] The lack of a counterion implies intramolecular charge compensation and therefore mixed-valence character for $[Fe^{II}Fe^{III}_2O(L^2)_3(OAc)_3]$ (**4**).

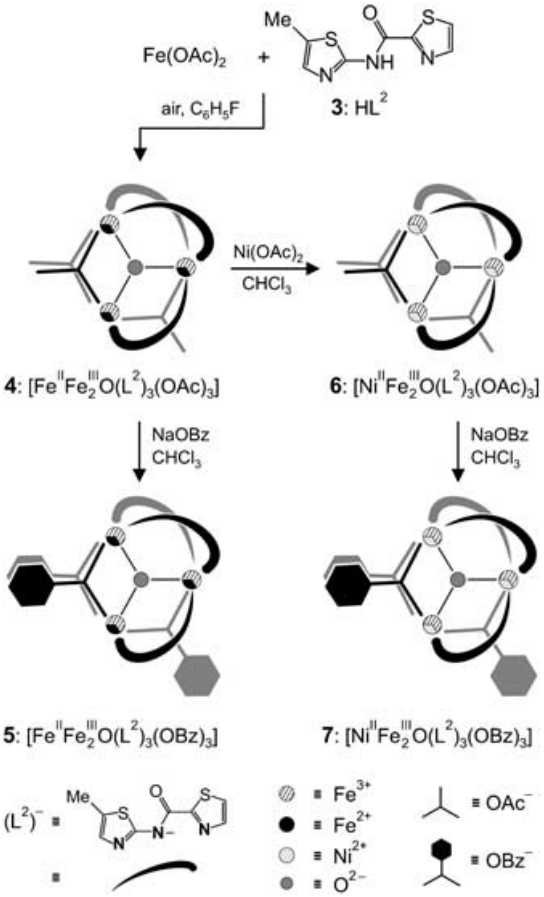

Scheme 3. Synthesis and schematic presentation of homotrinuclear $[Fe^{II}Fe^{III}_2O(L^2)_3(OAc)_3]$ (**4**) and $[Fe^{II}Fe^{III}_2O(L^2)_3(OBz)_3]$ (**5**); and heterotrinuclear $[Ni^{II}Fe^{III}_2O(L^2)_3(OAc)_3]$ (**6**) and $[Ni^{II}Fe^{III}_2O(L^2)_3(OBz)_3]$ (**7**).

X-ray structure analysis: However, these analytical data alone did not unequivocally confirm the structure of **4**. Since all our efforts to grow single crystals suitable for an X-ray structure analysis of **4** were unsuccessful, we generated $[Fe^{II}Fe^{III}_2O(L^2)_3(OBz)_3]$ (**5**) from **4** by exchange of the $(OAc)^-$ co-ligands with $(OBz)^-$ ions (Scheme 3). In contrast to **4**, crystals of **5** were readily available when diethyl ether was allowed to evaporate into a solution of **5** in chloroform. According to the single-crystal X-ray structure determination,[7–9] $[Fe^{II}Fe^{III}_2O(L^2)_3(OBz)_3]$ (**5**) is made up of three ditopic, tridentate ligands $(L^2)^-$ and three bridging benzoate co-ligands, which fix the $Fe^{II}Fe^{III}_2$ ions in the corners of a triangle with an μ_3-O^{2-} ion in the center (mean distance Fe–μ_3-O = 1.88 Å). The iron centers Fe1/2 are linked by two $(L^2)^-$ ligands (head-to-tail/tail-to-head), Fe2/3 by one $(L^2)^-$ ligand (head-to-tail) and a benzoate ion, and Fe1/3 by two benzoate bridges. As a consequence, all three iron ions in the mixed-valent complex $[Fe^{II}Fe^{III}_2O(L^2)_3(OBz)_3]$ (**5**) are differently octahedrally coordinated (Figure 1).

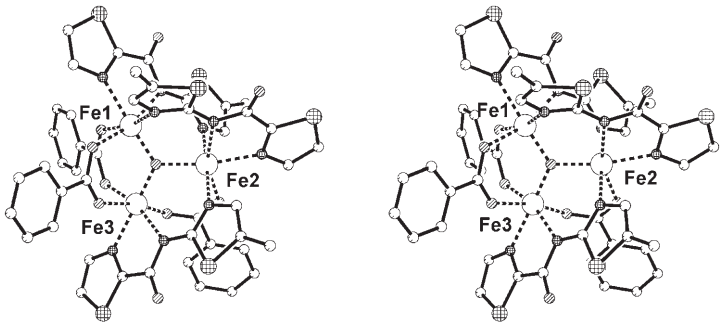

Figure 1. Molecular structure of **5** in the crystal (Stereoview, PLUTON presentation, with the numbering of the iron ions, only one stereoisomer shown). H atoms omitted for clarity. C: shaded; N: net; O: diagonal; S: mesh; Fe: void.

Variable-temperature Mössbauer studies: To further support the mixed-valent character of the unprecedented *asymmetrically* substituted **4** and **5**, and to gain deeper insight into the electron-exchange processes of these μ_3-oxo-triiron complexes, we carried out variable-temperature Mössbauer measurements of powder samples of both complexes (Figure 2, Table 1).

The Mössbauer spectra of **4** and **5** at 300 K are almost identical and both exhibit two quadrupolar doublets with an area ratio of 1:2 for the Fe^{II} and the two Fe^{III} ions. The doublet with a quadrupole splitting of $\Delta E_Q = 1.59(3)$ mms^{-1} (**4**), 1.43(3) mms^{-1} (**5**) and an isomeric shift of $\delta = 0.97(3)$ mms^{-1} (**4**), 0.89(3) mms^{-1} (**5**) is consistent with a high-spin iron(II) species (relative intensity: 33(3)%), whereas the doublet with a quadrupole splitting of $\Delta E_Q = 1.18(3)$ mms^{-1} (**4**, **5**) and an isomeric shift of $\delta = 0.43(3)$ mms^{-1} (**4**), 0.46 (3) mms^{-1} (**5**) is consistent with a high-spin iron(III) species (relative intensity: 67(3)%).

Most interestingly, at 4.2 K the Mössbauer spectra of **4** and **5** differ considerably (Figure 2, Table 1). The spectrum

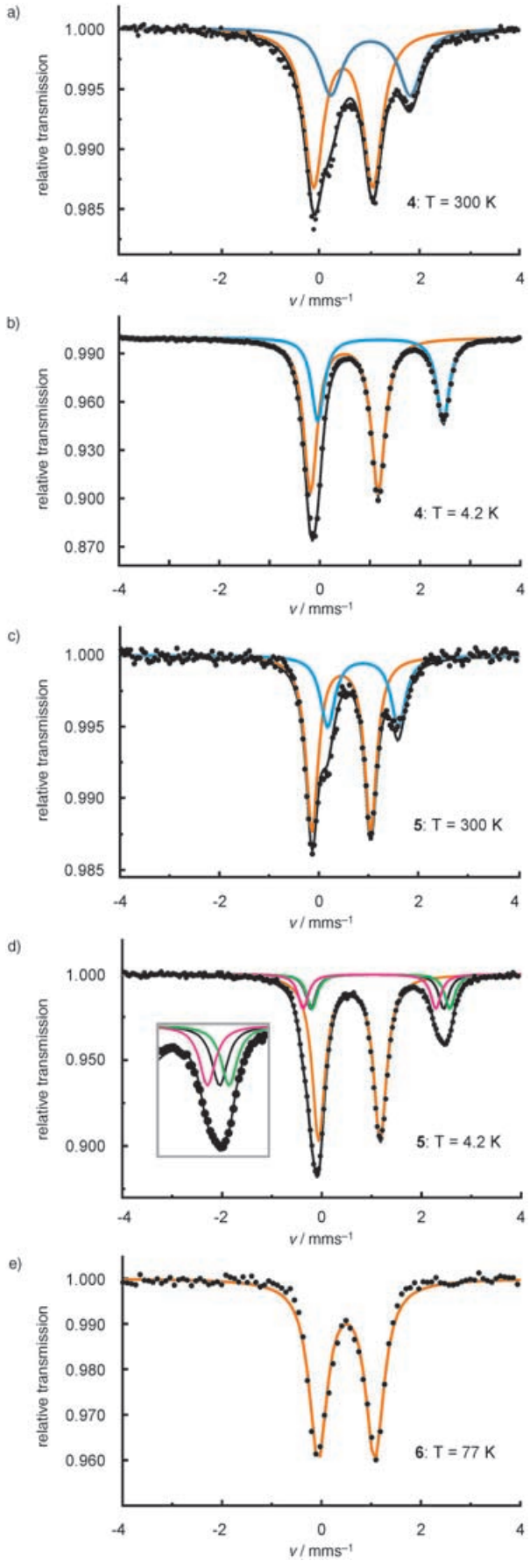

Figure 2. Mössbauer spectra of **4** (a: 300 K; b: 4.2 K), **5** (c: 300 K; d: 4.2 K), and **6** (e: 77 K). The orange and blue solid lines are Lorentzian fits for the iron(III) and iron(II) centers, respectively. For **5**, the experimental data at 4.2 K of the three differently substituted high-spin Fe^{II} centers are best fitted by three individual quadrupole doublets, the high-velocity lines of which are highlighted in the inset of (d) in magenta, black, and green.

Table 1. Parameters obtained from the analysis of the Mössbauer spectra of complexes **4**–**7**.[a]

	Complex	T [K]	δ [mm s^{-1}]	ΔE_Q [mm s^{-1}]	Γ [mm s^{-1}]	Rel. area [%]
4	Fe^{III}	300	0.43(3)	1.18(3)	0.46(3)	67(3)
	Fe^{II}		0.97(3)	1.59(3)	0.54(3)	33(3)
	Fe^{III}	4.2	0.49(2)	1.35(2)	0.32(2)	66(2)
	Fe^{II}		1.21(2)	2.50(2)	0.30(2)	33(2)
5	Fe^{III}	300	0.46(3)	1.18(3)	0.29(3)	67(3)
	Fe^{II}		0.89(3)	1.43(3)	0.35(3)	33(3)
	Fe^{III}	4.2	0.56(2)	1.23(2)	0.31(2)	67(2)
	Fe^{II}		1.19(2)	2.77(2)	0.25(2)	11(1)
	Fe^{II}		1.12(2)	2.66(2)	0.25(2)	11(1)
	Fe^{II}		0.96(2)	2.66(2)	0.25(2)	11(1)
6	Fe^{III}	77	0.50(2)	1.14(2)	0.44(2)	100
7	Fe^{III}	77	0.49(2)	1.21(2)	0.41(2)	100

[a] Errors in the last digit are given in brackets.

of **4** at 4.2 K was fitted with two doublets, yielding reasonably narrow line widths Γ and an area ratio of 1:2 for the Fe^{II} and the two Fe^{III} ions ($\Delta E_Q = 2.50(2)$ mms^{-1}, $\delta = 1.21(2)$ mms^{-1}, $\Gamma = 0.30(2)$ mms^{-1} for Fe^{II} and $\Delta E_Q = 1.35(2)$ mms^{-1}, $\delta = 0.49(2)$ mms^{-1}, $\Gamma = 0.32(2)$ mms^{-1} for Fe^{III}). The Fe^{II} site in **5** exhibits a stronger temperature dependence of the quadrupole splitting than in **4**, indicating that the energy splitting of the t_{2g} shell is smaller in **5** than in **4**. This is consistent with a somewhat stronger distortion of the axial ligand field at the Fe^{II} site in **5** compared to that in **4**. Unlike for **4**, the spectrum at 4.2 K for **5** shows a rather broad signature of the Fe^{II} doublet as compared with the Fe^{III} doublet: whereas the lines of the quadrupole doublet for the two Fe^{III} ions are sharp ($\Delta E_Q = 1.23(2)$ mms^{-1}, $\delta = 0.56(2)$ mms^{-1}, $\Gamma = 0.31(2)$ mms^{-1}, 67(2)%), the lines of the quadrupole doublet of Fe^{II} are rather broad (~0.65 mms^{-1}). The experimental data are best fitted by three doublets ($\Delta E_Q = 2.77(2)$, 2.66(2), 2.66(2) mms^{-1}; $\delta = 1.19(2)$, 1.12(2), 0.96(2) mms^{-1}; $\Gamma = 0.25(2)$, 0.25(2), 0.25(2) mms^{-1}), which represent Fe^{II} with a relative area ratio of 11(1), 11(1), and 11(1)%, respectively.

Although the ferric site of **5** exhibits a marginally higher isomer shift of 0.56(2) mms^{-1} than the ferric site of **4** (0.49(2) mms^{-1}), we exclude the presence of partial electron delocalization[10] at 4.2 K, since the all-ferric complexes **6** and **7** show comparable values at 77 K ($\delta = 0.50(2)$ and 0.49(2) mms^{-1}, Table 1).

The effect of the $(OAc)^-$ co-ligands on the ($Fe^{II}Fe^{III}_2$) core in **4** obviously is different from the effect of the $(OBz)^-$ co-ligands on the iron core in **5**, leading to the situation that in **5**, the difference in coordination among iron sites is larger

than in **4**. This is consistent with the observed stronger temperature dependence of the quadrupole splitting at Fe^{II} sites in **5** than in **4**. In addition, the exchange of $(OAc)^-$ co-ligands with $(OBz)^-$ co-ligands could also influence electron-exchange rates, electronic couplings, or local vibronic couplings, thus affecting also activation barriers. Comparison of the Mössbauer data at 4.2 K and 300 K reveals a larger increase of line broadening for all iron sites at 300 K in **4** than for the same sites in **5**. From this finding it seems that (thermally activated) electron exchange is faster and gets closer to the Mössbauer time window in **4** than in **5**. As a result of the different coordination of the iron sites [(Fe1)3N/3O, (Fe2)4N/2O, (Fe3)2N/4O], there exist evidently three configurations with unlike energies $[(Fe1)^{II}(Fe2)^{III}(Fe3)^{III}$, $(Fe1)^{III}(Fe2)^{II}(Fe3)^{III}$, $(Fe1)^{III}(Fe2)^{III}(Fe3)^{II}]$ for **4** and **5**. Even if the difference among these energies is small and can be overcome at elevated temperature by thermal activation, at low temperature one expects that only the configuration with the lowest energy is populated, corresponding to only one Fe^{II} doublet in the Mössbauer spectrum at 4.2 K. From ligand field theoretical considerations the configuration with the lowest energy is Fe^{II} with a 4N/2O core. However, assuming a slow electron-tunneling exchange mechanism in **5**, one might arrive at a situation, at which all three configurations remain nearly equally populated, even at very low temperature. Since the differences in coordination affect more significantly the Mössbauer characteristics of Fe^{II} than of Fe^{III}, the slow exchange and the three different types of coordination explain the presence of three Fe^{II} doublets and of only one Fe^{III} doublet at 4.2 K in **5**. Such a situation is not unlikely. We and others have found molecular subconfigurations of iron proteins at low temperature by Mössbauer spectroscopy[11,12] and optical methods;[13] these subconfigurations exist simultaneously and give rise to low-temperature molecular dynamics extending over months.[12]

Within this picture, electron exchange in **4** is fast enough to populate only the lowest energy configuration at low temperature. At 300 K thermal fluctuations equalize the ligand field strength around each iron site in **4** and **5**, such that it is not possible to resolve the different $(Fe1)^{II}$, $(Fe2)^{II}$, and $(Fe3)^{II}$ components in the Mössbauer spectra.

Exchange of Fe^{II} by Ni^{II}: To provide further insight into the electronic structure of **4** and **5**, we prepared the heteronuclear, mixed-valent cluster $[Ni^{II}Fe_2^{III}O(L^2)_3(OAc)_3]$ (**6**), by exchanging Fe^{II} in the mixed-valent all-iron complex **4** with Ni^{II} by using an excess of nickel acetate (Scheme 3). Complete Fe^{II}-to-Ni^{II} exchange in **4** was established unequivocally from the Mössbauer spectrum of **6** at 77 K (Figure 2, Table 1). Powder samples of **6** displayed a rather sharp single quadrupolar doublet (two high-spin Fe^{III} centers: $\Delta E_Q(77\,K) = 1.14\ mms^{-1}$, $\delta(77\,K) = 0.50\ mms^{-1}$, $\Gamma = 0.44\ mms^{-1}$, 100 %).

Again, we were not able to grow single crystals suitable for an X-ray structure analysis of **6**. Therefore, we generated $[Ni^{II}Fe_2^{III}O(L^2)_3(OBz)_3]$ (**7**) from **6** by exchange of the $(OAc)^-$ co-ligands with $(OBz)^-$ ions (Scheme 3). Compared with **6**, complex **7** displayed a similar Mössbauer spectrum (Table 1, Figure 2). The X-ray structure analysis of **7**[14] revealed it to be isostructural with **5**.

Cyclic voltammetry: The reversible cyclic voltammograms[15] of redox-active **4** and **5** were recorded under anaerobic, aprotic conditions, and displayed basically two processes attributable to the reduction of **4** and **5** from $Fe^{II}Fe_2^{III}$ to $Fe_2^{II}Fe^{III}$, and oxidation to the all-Fe^{III} species (Figure 3, Table 2). The number of electrons transferred at different

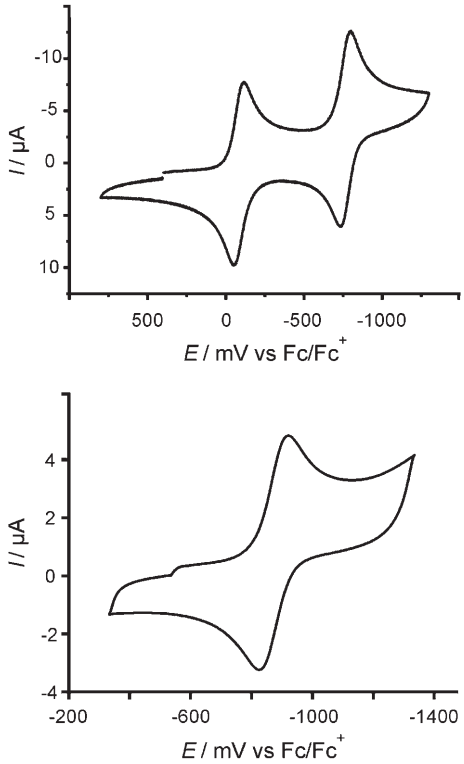

Figure 3. Cyclic voltammograms of **5** (top) and **7** (bottom).

potentials during this process was determined in acetonitrile versus Fc/Fc^+ and turned out to be one for the reduction of all-Fe^{III} to $Fe^{II}Fe_2^{III}$ and one for the second reduction to

Table 2. Half-wave potential ($E_{1/2}$) values of complexes **4**–**7**.[a]

Complex	**4**	**5**	**6**	**7**
$E^1_{1/2}$ [mV]	−151	−85		
$E^2_{1/2}$ [mV]	−837	−765	−939	−872

[a] Recorded in CH_3CN (0.1 M $[(n\text{Bu})_4N][PF_6]$) versus Fc/Fc^+ at 20 °C; scan rate 200 mVs^{-1}.

$Fe_2^{II}Fe^{III}$. Further reduction of $Fe_2^{II}Fe^{III}$ to the all-Fe^{II} species is irreversible. Consequently, the cyclic voltammograms of redox-active **6** and **7** represent the reduction of $Ni^{II}Fe_2^{III}$ to $Ni^{II}Fe^{II}Fe^{III}$, and reoxidation to $Ni^{II}Fe_2^{III}$ (Figure 3, Table 2). As determined in acetonitrile versus Fc/Fc^+, one electron is

transferred during this redox process. Further reduction of $Ni^{II}Fe^{II}Fe^{III}$ to the $Ni^{II}Fe^{II}_2$ species is irreversible.

Conclusion

In summary, we have presented a new synthesis of homo-/heterotrinuclear mixed-valent oxo-centered heteroleptic species that are structurally related to the active sites of numerous iron–oxo proteins. Variable-temperature Mössbauer spectroscopy of $[Fe^{II}Fe^{III}_2O(L^2)_3(OAc)_3]$ (**4**) calls for the occurrence of fast electron exchange and population of only one of the three configurations of **4** at 4.2 K, whereas, for $[Fe^{II}Fe^{III}_2O(L^2)_3(OBz)_3]$ (**5**) at 4.2 K slow electron exchange leads to almost equal population within the three unlike substituted iron sites in **5**. Obviously, the effect of the $(OAc)^-$ co-ligands on the $(Fe^{II}Fe^{III}_2)$ core in **4** is weaker than the effect of the $(OBz)^-$ co-ligands on the iron core in **5**. As demonstrated by cyclovoltammetry for **4** and **5**, the redox-active chelate complexes are stable for Fe^{III}_3, $Fe^{II}Fe^{III}_2$, and $Fe^{II}_2Fe^{III}$ but not for Fe^{II}_3.

Experimental Section

General methods and materials: All reagents and solvents employed were commercially available high-grade purity materials (Fluka, Aldrich), used as supplied without further purification. IR spectra were recorded from $CHBr_3$ triturations on a Bruker IFS 25 spectrometer. FAB-MS spectra were recorded on a Micromass ZAB-Spec spectrometer. Elemental analyses were performed on a EA 1110 CHNS-Microautomat. The microanalytical data for **4** and **6** deviate from theory due to the presence of crystal solvents and are not recorded here.

Cyclic voltammetry:[15] Cyclic voltammetry at a platinum electrode was performed in CH_3CN/TBAH (0.2 M, TBAH = $[(n\text{Bu})_4\text{N}][PF_6]$) at room temperature under an argon atmosphere using a three-electrode set-up and an EG&G (potentiostat/galvanostat) model 283. Redox potentials were internally referenced against ferrocene/ferrocenium (Fc/Fc^+). HPLC-grade CH_3CN for electrochemical experiments was refluxed and distilled over CaH_2 under a nitrogen atmosphere. Tetra-*n*-butylammonium hexafluorophosphate was prepared and purified according to a previously described procedure.[16]

$[Fe^{II}Fe^{III}_2O(L^2)_3(OAc)_3]$ (4): A solution of HL^2 **3** (135 mg, 0.6 mmol) in fluorobenzene (15 mL) was added to a suspension of iron(II) acetate (87 mg, 0.5 mmol) in fluorobenzene (35 mL). The reaction mixture was stirred at 20 °C for 24 h in the presence of air. After addition of five drops of distilled water, stirring was continued for a further 24 h. The precipitate was collected and dried under reduced pressure. Yield: 102 mg (59 %) dark violet powder; m.p. > 250 °C (decomp); IR (KBr): $\tilde{\nu}$ = 3132, 2919, 1609, 1568, 1556, 1504 cm^{-1}; FAB-MS (*m*-NBA): *m*/*z* (%): 1033 (52) $[M]^+$, 974 (100) $[M-OAc]^+$, 915 (48) $[M-2OAc]^+$, 856 (21) $[M-3OAc]^+$, 809 (40) $[M-L^2]^+$, 750 (59) $[M-OAc-L^2]^+$, 691 (55) $[M-2OAc-L^2]^+$, 576 (86) $[M-3OAc-L^2-Fe]^+$, 526 (31) $[M-OAc-2L^2]^+$; $C_{30}H_{27}Fe_3N_9O_{10}S_6$ (1033.50).

$[Fe^{II}Fe^{III}_2O(L^2)_3(OBz)_3]$ (5): Sodium benzoate (692 mg, 4.8 mmol) was added to a solution of **4** (83 mg, 0.08 mmol) in chloroform (25 mL). The pale violet suspension was stirred at 20 °C for 48 h. After removal of excess of the sodium salt, the remaining solution was evaporated to dryness. Yield: 67 mg (69 %) dark violet crystals from $CHCl_3$ by vapor diffusion of diethyl ether; m.p. > 250 °C (decomp); IR (KBr): $\tilde{\nu}$ = 3120, 3104, 3061, 2920, 1597, 1560, 1505 cm^{-1}; FAB-MS (*m*-NBA): *m*/*z* (%): 1219 (100) $[M]^+$, 1098 (74) $[M\text{-}OBz]^+$, 995 (86) $[M-L^2]^+$, 874 (49) $[M-OBz-L^2]^+$, 771 (33) $[M-2L^2]^+$, 753 (23) $[M-2OBz-L^2]^+$, 650 (40) $[M-2L^2-OBz]^+$, 576 (46) $[M-3OBz-L^2-Fe]^+$; elemental analysis calcd (%) for $C_{45}H_{33}Fe_3N_9O_{10}S_6 \cdot 0.5\ CHCl_3$ (1279.40): C 42.72, H 2.64, N 9.85; found: C 42.72, H 2.80, N 9.78.

$[Ni^{II}Fe^{III}_2O(L^2)_3(OAc)_3]$ (6): Nickel acetate tetrahydrate (93 mg, 0.375 mmol) was added to a solution of **4** (78 mg, 0.075 mmol) in chloroform (15 mL). The initially violet suspension was stirred at 20 °C for 48 h. After filtration over a pad of celite, the remaining brown solution was evaporated to dryness. Yield: 43 mg (55 %) brown precipitate from $CHCl_3$/*n*-pentane (5 mL/30 mL, 2×); m.p. > 250 °C (decomp); IR (KBr): $\tilde{\nu}$ = 2926, 2855, 1614, 1568, 1556, 1505 cm^{-1}; FAB-MS (*m*-NBA): *m*/*z* (%): 1035 (10) $[M]^+$, 976 (69) $[M-OAc]^+$, 917 (13) $[M-2OAc]^+$, 811 (100) $[M-L^2]^+$, 788 (24), 752 (47) $[M-OAc-L^2]^+$, 693 (21) $[M-2OAc-L^2]^+$, 528 (28) $[M-OAc-2L^2]^+$; $C_{30}H_{27}Fe_2N_9NiO_{10}S_6$ (1036.36).

$[Ni^{II}Fe^{III}_2O(L^2)_3(OBz)_3]$ (7): In analogy to compound **5**, **6** (62 mg, 0.06 mmol) was allowed to react with sodium benzoate (519 mg, 3.6 mmol) in chloroform (20 mL). Yield: 45 mg (61 %) deep brown crystals from $CHCl_3$ by vapor diffusion of diethyl ether; m.p. > 250 °C (decomp); IR (KBr): $\tilde{\nu}$ = 3113, 3086, 2921, 1600, 1565, 1551, 1504 cm^{-1}; FAB-MS (*m*-NBA): *m*/*z* (%): 1222 (17) $[M+H]^+$, 1100 (100) $[M-OBz]^+$, 997 (80) $[M-L^2]^+$, 979 (18) $[M-2OBz]^+$, 876 (37) $[M-OBz-L^2]^+$, 773 (20) $[M-2L^2]^+$, 755 (14) $[M-2OBz-L^2]^+$, 652 (19) $[M-2L^2-OBz]^+$, 578 (18) $[M-3OBz-L^2-Fe]^+$; elemental analysis calcd (%) for $C_{45}H_{33}Fe_2N_9NiO_{10}S_6 \cdot CHCl_3$ (1341.95): C 41.17, H 2.55, N 9.39; found: C 40.86, H 2.87, N 9.83.

Acknowledgements

We thank one of the referees for valuable advice. Generous financial support by the Deutsche Forschungsgemeinschaft Sa 276/27–1, SFB 583, GK 312, SPP 1137, the Bayerisches Langzeitprogramm Neue Werkstoffe, and the Fonds der Chemischen Industrie are gratefully acknowledged. We also would like to thank cand.-chem. Ignacio Ferrero Veyrat for his help supported by an ERASMUS Fellowship.

[1] Recent reviews: a) B. J. Holliday, C. A. Mirkin, *Angew. Chem.* **2001**, *113*, 2076–2097; *Angew. Chem. Int. Ed.* **2001**, *40*, 2022–2043; b) S. R. Seidel, P. J. Stang, *Acc. Chem. Res.* **2002**, *35*, 972–983; c) R. W. Saalfrank, B. Demleitner, in *Transition Metals in Supramolecular Chemistry* (Ed.: J. P. Sauvage), Wiley-VCH, Weinheim, **1999**, p. 1–51; d) E. Uller, B. Demleitner, I. Bernt, R. W. Saalfrank, *Struct. Bonding* **2000**, *96*, 149–175; e) D. L. Caulder, K. N. Raymond, *Acc. Chem. Res.* **1999**, *32*, 975–982; f) J. L. Atwood, L. R. MacGillivray, *Angew. Chem.* **1999**, *111*, 1080–1096; *Angew. Chem. Int. Ed.* **1999**, *38*, 1018–1033; g) M. Fujita, *Chem. Soc. Rev.* **1998**, *27*, 417–425; h) C. J. Jones, *Chem. Soc. Rev.* **1998**, *27*, 289–299; i) C. Piguet, G. Bernardinelli, G. Hopfgartner, *Chem. Rev.* **1997**, *97*, 2005–2062; j) G. F. Swiegers, T. J. Malefetse, *Coord. Chem. Rev.* **2002**, *225*, 91–121.

[2] a) R. Sessoli, D. Gatteschi, *Angew. Chem.* **2003**, *115*, 278–309; *Angew. Chem. Int. Ed.* **2003**, *42*, 268–297; b) C. Benelli, A. J. Blake, E. K. Brechin, S. J. Coles, A. Graham, S. G. Harris, S. Meier, A. Parkin, S. Parson, A. M. Seddon, R. E. P. Winpenny, *Chem. Eur. J.* **2000**, *6*, 883–896; c) O. Waldmann, J. Schülein, R. Koch, P. Müller, I. Bernt, R. W. Saalfrank, H. P. Andres, H. U. Güdel, P. Allenspach, *Inorg. Chem.* **1999**, *38*, 5879–5886; d) O. Waldmann, R. Koch, S. Schromm, P. Müller, I. Bernt, R. W. Saalfrank, *Phys. Rev. Lett.* **2002**, *89*, 246401–1–4; e) A. Cornia, A. C. Fabretti, P. Garrisi, C. Mortalò, D. Bonacchi, D. Gatteschi, R. Sessoli, L. Sorace, W. Wernsdörfer, A.-L. Barra, *Angew. Chem.* **2004**, *116*, 1156–1159; *Angew. Chem. Int. Ed.* **2004**, *43*, 1136–1139; f) V. Marvaud, C. Decroix, A. Scuiller, C. Guyard-Duhayon, J. Vaisermann, J. Gonnet, M. Verdaguer, *Chem. Eur. J.* **2003**, *9*, 1677–1691.

[3] R. W. Saalfrank, S. Trummer, U. Reimann, M. M. Chowdhry, F. Hampel, O. Waldmann, *Angew. Chem.* **2000**, *112*, 3634–3637; *Angew. Chem. Int. Ed.* **2000**, *39*, 3492–3494.

[4] R. W. Saalfrank, U. Reimann, M. Göritz, F. Hampel, A. Scheurer, F. W. Heinemann, M. Büschel, J. Daub, V. Schünemann, A. X. Trautwein, *Chem. Eur. J.* **2002**, *8*, 3614–3619.

[5] Complex **4** is only generated with fresh $Fe(OAc)_2$ (Supplier Aldrich 51,793–3; 99,995%), whereas aged $Fe(OAc)_2$ (kept under nitrogen in a Schlenk tube for 6–9 months with occasional opening) leads to $[\{Fe^{III}_3O(L^2)_2(OAc)_4\}_2O]$ (**I**), described in reference [4]. Small amounts of complex **I** could be isolated from a solution of **4** in chloroform that was left to stand for several days.

[6] For further iron acetate complexes see: a) C. T. Dziobkowski, J. T. Wrobelski, D. B. Brown, *Inorg. Chem.* **1981**, *20*, 671–678; b) C. J. Harding, R. K. Henderson, A. K. Powell, *Angew. Chem.* **1993**, *105*, 583–585; *Angew. Chem. Int. Ed. Engl.* **1993**, *32*, 570–572; c) C. A. Christmas, H.-L. Tsai, L. Pardi, J. M. Kesselman, P. K. Gantzel, R. K. Chadha, D. Gatteschi, D. F. Harvey, D. N. Hendrickson, *J. Am. Chem. Soc.* **1993**, *115*, 12483–12490; d) I. Shwey, L. E. Pence, G. C. Papaefthymiou, R. Sessoli, J. W. Yun, A. Bino, S. J. Lippard, *J. Am. Chem. Soc.* **1997**, *119*, 1037–1042; e) S. J. Lippard, *Angew. Chem.* **1988**, *100*, 353–371; *Angew. Chem. Int. Ed. Engl.* **1988**, *27*, 344–361; f) S. G. Sreerama, S. Pal, *Eur. J. Inorg. Chem.* **2004**, 4718–4723.

[7] Crystal data for $[Fe^{II}Fe^{III}_2O(L^2)_3(OBz)_3]$ (**5**): $C_{45}H_{33}Fe_3N_9O_{10}S_6\cdot 2.5\,CHCl_3$, $M_r=1518.13$; crystal dimensions $0.30\times0.20\times0.20\,mm^3$; triclinic, space group $P\bar{1}$, $a=13.9564(1)$, $b=14.0938(1)$, $c=17.8277(1)$ Å, $\alpha=93.535(1)$, $\beta=95.976(1)$, $\gamma=115.950(1)°$, $V=3113.37(4)$ Å^3; $Z=2$; $F(000)=1530$, $\rho_{calcd}=1.619\,g\,cm^{-3}$; diffractometer: Nonius KappaCCD, $Mo_{K\alpha}$ radiation ($\lambda=0.71073$ Å); $T=173(2)$ K; graphite monochromator; theta range [°] $2.04<\theta<27.52$; section of the reciprocal lattice: $-18\le h\le18$, $-18\le k\le18$, $-23\le l\le23$; of 27053 measured reflections, 14270 were independent and 10803 with $I>2\sigma(I)$; linear absorption coefficient $1.273\,mm^{-1}$. The structure was solved by direct methods using SHELXS-97 and refinement with all data (766 parameters) by full-matrix least-squares on F^2 using SHELXL97;[8] all non-hydrogen atoms were refined anisotropically; $R1=0.0581$ for $I>2\sigma(I)$ and $wR2=0.1865$ (all data); largest peak (1.15 eÅ^{-3}) and hole (-1.148 eÅ^{-3}).[8,9]

[8] a) G. M. Sheldrick, C. Krüger, P. Goddard, *Crystallographic Computing 3*, Oxford University Press, Oxford **1985**, p. 175; b) G. M. Sheldrick, SHELXL-97, *program for crystal structure refinement*, University of Göttingen **1997**.

[9] CCDC-205798 (**5**), and CCDC-205799 (**7**) contain the supplementary crystallographic data for this paper. These data can be obtained free of charge from the Cambridge Crystallographic Data Centre via www.ccdc.cam.ac.uk/data_request/cif.

[10] Cf.: a) R. W. Saalfrank, S. Trummer, H. Krautscheid, V. Schünemann, A. X. Trautwein, S. Hien, C. Stadler, J. Daub, *Angew. Chem.* **1996**, *108*, 2350–2352; *Angew. Chem. Int. Ed. Engl.* **1996**, *35*, 2206–2208; b) C. Stadler, J. Daub, J. Köhler, R. W. Saalfrank, V. Coropceanu, V. Schünemann, C. Ober, A. X. Trautwein, S. F. Parker, M. Poyraz, T. Inomata, R. Cannon, *J. Chem. Soc. Dalton Trans.* **2001**, 3373–3383; c) C. Wilson, B. B. Iversen, J. Overgaard, F. K. Larsen, G. Wu, S. P. Palii, G. A. Timco, N. V. Gerbeleu, *J. Am. Chem. Soc.* **2000**, *122*, 11370–11379; d) J. Overgaard, F. K. Larsen, B. Schiøtt, B. B. Iversen, *J. Am. Chem. Soc.* **2003**, *125*, 11088–11099.

[11] C. Ober, M. Burkhardt, H. Winkler, A. X. Trautwein, A. A. Zharikov, S. F. Fischer, F. Parak, *Eur. Biophys. J.* **1997**, *26*, 227–237.

[12] H. Frauenfelder, F. Parak, R. D. Young, *Annu. Rev. Biophys. Biophys. Chem.* **1988**, *17*, 451–479.

[13] H. Winkler, M. Franke, A. X. Trautwein, F. Parak, *Hyperfine Interact.* **1990**, *58*, 2405–2412.

[14] Crystal data for $[Ni^{II}Fe^{III}_2O(L^2)_3(OBz)_3]$ (**7**): $C_{45}H_{33}Fe_2N_9NiO_{10}S_6\cdot 2\,CHCl_3$, $M_r=1461.31$; crystal dimensions $0.30\times0.20\times0.20\,mm^3$; triclinic, space group $P\bar{1}$, $a=13.9543(2)$, $b=14.1362(2)$, $c=17.8070(4)$ Å, $\alpha=93.661(1)$, $\beta=95.761(1)$, $\gamma=116.753(1)°$, $V=3097.18(9)$ Å^3; $Z=2$; $F(000)=1476$, $\rho_{calcd}=1.567\,g\,cm^{-3}$; diffractometer: Nonius KappaCCD, $Mo_{K\alpha}$ radiation ($\lambda=0.71073$ Å); $T=173(2)$ K; graphite monochromator; theta range [°] $1.16<\theta<27.79$; section of the reciprocal lattice: $-17\le h\le17$, $-17\le k\le18$, $-21\le l\le22$; of 22533 measured reflections, 13700 were independent and 7900 with $I>2\sigma(I)$; linear absorption coefficient $1.214\,mm^{-1}$. The structure was solved by direct methods using SHELXS-97 and refinement with all data (734 parameters) by full-matrix least-squares on F^2 using SHELXL97;[8] all non-hydrogen atoms were refined anisotropically; $R1=0.0816$ for $I>2\sigma(I)$ and $wR2=0.2522$ (all data); largest peak (1.834 eÅ^{-3}) and hole (-1.102 eÅ^{-3}).[8,9]

[15] M. Büschel, C. Stadler, Ch. Lambert, M. Beck, J. Daub, *J. Electroanal. Chem.* **2000**, *484*, 24–32.

[16] J. Salbeck, PhD thesis, Universität Regensburg (Germany), **1988**, p. 196.

Received: January 27, 2005
Published online: July 25, 2005

